UDC 004.7 + 007.5
DOI: 10.15587/1729-4061.2026.352116

OPTIMIZATION OF CHANNEL PACKET LOSS IN WIRELESS SENSOR COMMUNICATION SYSTEMS USING MODEL PREDICTIVE CONTROL

Ainur Ormanbekova
Doctor of Philosophy (PhD), Assistant Professor, Dean of Faculty
Department of Engineering and Information Technology***
ORCID: https://orcid.org/0000-0001-8663-006X
Anar Khabay
Corresponding author
Doctor PhD, Associate Professor*
E-mail: a.khabay@satbayev.university
ORCID: https://orcid.org/0000-0002-0409-1531
Yerkebulan Tuleshov
Candidate of Technical Sciences, Associate Professor
Department of Robotics and Technical Means of Automation**
ORCID: https://orcid.org/0000-0002-9146-7137
Nurlan Sarsenbayev
Candidate of Technical Sciences, Associate Professor
Department of Automation and Control**
ORCID: https://orcid.org/0000-0001-8640-7175
Zhazira Julayeva
Master of Technical Sciences
Department of Automation and Robotics***
ORCID: https://orcid.org/0000-0001-9246-3851
Serikbek Ibekeyev
Master of Technical Sciences, Senior Lecturer
Department of Computer Engineering***
ORCID: https://orcid.org/0000-0002-1991-8642
Maral Abulkhanova
Senior Lecturer*
ORCID: https://orcid.org/0000-0001-6055-1646
Askhat Tlegenov
Master Student of Technical Sciences*
ORCID: https://orcid.org/0009-0006-0967-1443
Magzhan Igen
Master's Student in Telecommunications**
ORCID: https://orcid.org/0009-0006-7156-5182
*Department of Electronics, Telecommunications and Space Technology**
**Satbayev University
Satbayev str., 22, Almaty, Republic of Kazakhstan, 050013
***Almaty Technological University
Tole bi str., 100, Almaty, Republic of Kazakhstan, 050012

The object of the study is an IEEE 802.15.4 (2.4 GHz) wireless networked control system (WNCS) closing the loop over a wireless sensor network. Fading and interference increase packet loss and delay, reducing stability margins and control quality. The unresolved problem is the lack of a unified end-to-end (E2E) loss model that links PHY signal quality, multi-hop routing and medium access to closed-loop behavior and can be embedded into controller synthesis. An SINR-based channel model (path loss, lognormal shadowing, multipath fading) is mapped to BER and packet error probability; E2E loss for single-hop and multi-hop routes is obtained using Bernoulli and finite-state Markov (FSMC) processes. For verification, original packet traces are captured with an IEEE 802.15.4 sniffer/logger and stored before processing (timestamp, node identifier, sequence number, RSSI/LQI and delivery outcome) to compute PER, latency and burstiness and to parameterize the SINR-to-PER mapping and loss models. Simulations show that TDMA/TSCH achieves up to 40% lower loss than CSMA/CA, while E2E loss rises from 3% to 32% as hop count increases from 1 to 8. An MPC-based co-design jointly adapts transmit power, sampling period and retransmissions. Compared with a fixed-parameter LQR baseline, E2E PER is reduced from 4.45% to 3.66%, average delay from 0.20 s to 0.12 s, and integral absolute error by 50%. The gains are attributed to reduced contention under TDMA scheduling and predictor-driven MPC adaptation. The approach targets industrial monitoring and control with fixed sampling, slowly varying interference and static multi-hop topologies, where parameters can be identified offline and used for online MPC adaptation

Keywords: *wireless sensor network, WNCS, packet loss, SINR, Bernoulli process, finite-state Markov chain, TDMA, CSMA/CA, MPC*

Received 17.11.2025
Received in revised form 14.01.2026
Accepted 06.02.2026
Published 27.02.2026

How to Cite: *Ormanbekova, A., Khabay, A., Tuleshov, Y., Sarsenbayev, N., Julayeva, Z., Ibekeyev, S., Abulkhanova, M., Tlegenov, A., Igen, M. (2026). Optimization of channel packet loss in wireless sensor communication systems using model predictive control. Eastern-European Journal of Enterprise Technologies, 1 (9 (139)), 56–67. https://doi.org/10.15587/1729-4061.2026.352116*

1. Introduction

Because industrial facilities require continuous monitoring of technological processes, real-time data acquisition, and rapid supervisory control, the demand for massive wireless sensor connectivity that can simultaneously support large numbers of devices has intensified. In this context, industrial wireless sensor networks (IWSNs) are becoming one of the

key enabling infrastructures, as they can improve production efficiency, enable predictive maintenance, prevent emergency situations, and reduce resource consumption. Therefore, the industrial deployment of wireless sensor networks is currently highly relevant and closely aligned with modern digitalization requirements [1].

In industrial environments, wireless-channel interference, shadowing, and signal attenuation increase packet losses and induce random delays, which negatively affect control-system stability and transient response quality. Consequently, for widely adopted standards such as IEEE 802.15.4, accurately characterizing packet-loss behavior via physical-layer indicators such as the signal-to-interference-plus-noise ratio (SINR) and the resulting packet error rate (PER), and co-designing this characterization together with control algorithms, has become an important and timely research direction.

The IEEE 802.15.4 standard is among the most commonly used solutions for wireless networked control systems (WNCSs) and Internet of Things (IoT) applications. Recent studies have analyzed the MAC-layer operation of this standard using Markov-chain and queueing-theoretic models to evaluate key performance indicators such as throughput, delay, energy consumption, and packet-loss probability [2, 3]. However, many existing works focus primarily on protocol-level performance and do not fully reveal how packet losses and delays affect control quality in realistic industrial WNCS settings.

From a control-theoretic perspective, model predictive control (MPC) that explicitly accounts for network-induced effects (delays and packet losses) is widely regarded as a promising approach for networked control systems [4]. Several studies have shown that combining MPC with triggering strategies and protocol-level mechanisms can ensure system stability under network constraints and external disturbances [5, 6]. It has also been reported that predictive control methods for WNCS can preserve transient performance by compensating for packet delays and losses [7].

Nevertheless, recent years have highlighted that a unified and systematic framework is still insufficient – specifically, one that:

1) describes the IEEE 802.15.4-based wireless sensor channel with adequate accuracy using physical-layer indicators such as SINR and the corresponding PER;

2) enables this characterization to be jointly utilized with MPC-based control for WNCS.

Therefore, in industrial IEEE 802.15.4-based WNCSs, accurately identifying packet losses and delays and developing methods to mitigate their impact on control performance remains an urgent scientific and practical problem.

2. Literature review and problem statement

Data-driven identification of time-varying wireless channels has received significant attention in WNCS, particularly in scenarios where physical channel parameters are unavailable or hard to measure reliably. In this context, [8] presents a method for learning Markov models of fading channels and shows that WNCS performance over a WirelessHART link is close to that achievable with a physics-based stationary Markov formulation. The results highlight both the promise of data-driven modeling and the practical necessity of treating channel parameters as uncertain quantities that must be handled explicitly in reliability assessment and controller design.

At the MAC layer, [9] analyzes CSMA/CA contention in IEEE 802.15.4 and demonstrates that enhanced CSMA/CA contention efficiency (ECCE) can improve throughput and reduce delay via parameter optimization. Nevertheless, a complete analytical framework that explains reliability and loss under different traffic types and realistic interference, while also capturing contention-driven collisions, is still lacking. As a result, adaptive tuning of MAC parameters requires a more comprehensive loss/reliability model than what is commonly available.

Experimental evidence in [10] shows that packet losses in an IEEE 802.15.4-based WNCS exhibit bursty behavior, and that the Gilbert–Elliott model fits such traces with low error; it is also shown that Kalman filtering can mitigate the impact of losses and improve system behavior. However, the reported model does not fully incorporate hidden-terminal and collision effects that are inherent to contention-based access, and further validation on representative real setups is required. This motivates extending burst-loss models to include MAC-related collision mechanisms and evaluating them jointly with compensation methods such as filtering or forward error correction.

A separate line of the study emphasizes the role of interference. Results in [11, 12] confirm that as interference increases, reliability decreases and system performance can change significantly, implying that realistic interference modeling is essential for reliability assessment. Yet these studies are not specific to IEEE 802.15.4 and do not explicitly account for CSMA/CA collision dynamics; therefore, IEEE 802.15.4-oriented modeling must combine interference effects with contention/collision behavior within the same quantitative framework.

Time-varying probabilistic models of packet delivery are also reported in the literature. In [13], WSN performance is studied using a time-varying probabilistic delivery model. However, applying such a model directly to IEEE 802.15.4-based WNCS and linking it to closed-loop control performance remains open, because practical losses depend not only on time variation but also on load, interference, and MAC collisions. Hence, a time-varying yet protocol-aware delivery model is needed, together with explicit control-relevant metrics.

For multi-hop networks, [14] shows that losses arise not only from wireless channel errors but also from network-layer reliability issues such as node failures and topology/routing factors, and that end-to-end loss can accumulate with the number of hops. However, this work does not provide a full quantitative model and a mitigation method that can be directly applied to IEEE 802.15.4-based WNCS under varying routing and load conditions. Since multi-hop losses depend on routing, traffic, and topology dynamics, an end-to-end loss description that incorporates these effects remains necessary for WNCS-oriented design.

Finally, [15] reports co-design results for an IEEE 802.15.4-based WNCS under Wi-Fi interference and demonstrates that stable operation in certain scenarios requires joint consideration of network and control. At the same time, universal modeling rules and co-design procedures that remain valid under time-varying interference and MAC collisions across different industrial environments are not fully established, which motivates further development of integrated reliability-and-control evaluation methods.

Existing studies on IEEE 802.15.4-based industrial WNCS address key aspects mostly in isolation, including physical-layer propagation and SINR/PER modeling, MAC-layer performance (throughput, delay, collisions), multi-hop routing, and MPC-based control under packet losses and delays. However,

a unified and systematically validated end-to-end packet-loss and delay model is still lacking – one that simultaneously:

1) starts from physically interpretable SINR/BER-driven channel impairments and fading;

2) incorporates MAC-layer effects such as contention, collisions, and hidden-terminal behavior;

3) captures routing and topology effects in multi-hop networks;

4) links the resulting end-to-end reliability and delay description directly to controller synthesis.

The aim of this study is to develop and evaluate an integrated SINR-to-control co-design framework for IEEE 802.15.4-based WNCS.

3. The aim and objectives of the study

The aim of this study is to develop an integrated SINR-to-control co-design framework for IEEE 802.15.4 (2.4 GHz) wireless networked control systems (WNCS) that mitigates the impact of packet loss and communication delay on closed-loop control performance;

– to derive an IEEE 802.15.4-compliant SINR → BER → PER link reliability model and quantify link success probability as a function of distance and interference;

– to analyze and compare single-hop packet loss under TDMA/TSCH and CSMA/CA using Bernoulli and finite-state Markov chain (FSMC) loss models;

– to formulate and evaluate end-to-end packet loss in multi-hop networks and to derive a reliability-constrained traffic-splitting (co-design routing) rule that satisfies a given E2E loss requirement;

– to assess an MPC-based co-design procedure that jointly adapts WNCS communication parameters (transmit power, sampling/transmission period, and number of retransmissions) to satisfy reliability/delay constraints and improve closed-loop performance.

4. Materials and methods

4. 1. The object and hypothesis of the study

The object of the study is an IEEE 802.15.4 (2.4 GHz) wireless networked control system (WNCS) evaluated under both single-hop and multi-hop data delivery. The considered topologies include up to five nodes (denoted A–E) forming:

1) direct single-hop links;

2) a multi-hop routing path, as illustrated in Fig. 1.

The main hypothesis is that physical-layer reliability in an IEEE 802.15.4 (2.4 GHz) system can be characterized via SINR and an SINR → BER → PER mapping, and then transformed – while accounting for MAC-layer effects under TDMA/TSCH and CSMA/CA – into link-level and E2E predictors of packet loss and communication delay for both single-hop and multi-hop delivery. In this formulation, packet delivery outcomes are modeled either as independent Bernoulli losses or as temporally correlated losses using a finite-state Markov chain. Embedding these predictors into reliability-aware routing and wireless-aware model MPC enables joint adaptation of communication parameters (e.g., transmit power, sampling/transmission period, and number of retransmissions), thereby improving closed-loop stability and control performance under packet loss and network-induced delay.

In this study, during the experiment, IEEE 802.15.4 nodes labeled A–E are deployed in a 10 × 10 m area, and a scenario is executed in which each node transmits one packet every 5 s. Communication is evaluated under two modes: scheduled access (TDMA/TSCH) and contention-based access (CSMA/CA). During data collection, over-the-air frames are captured using an 802.15.4 packet sniffer and continuously stored by a logger on a laptop. Prior to any processing (without averaging or filtering), packet-level raw data are stored, including: timestamp, node identifier, packet sequence number, RSSI, LQI, and the delivery indicator $Xk \in \{0, 1\}$ (1 – delivered, 0 – lost); when latency is evaluated, the time stamps t_{tx} and t_{rx} (or their equivalents) are also recorded.

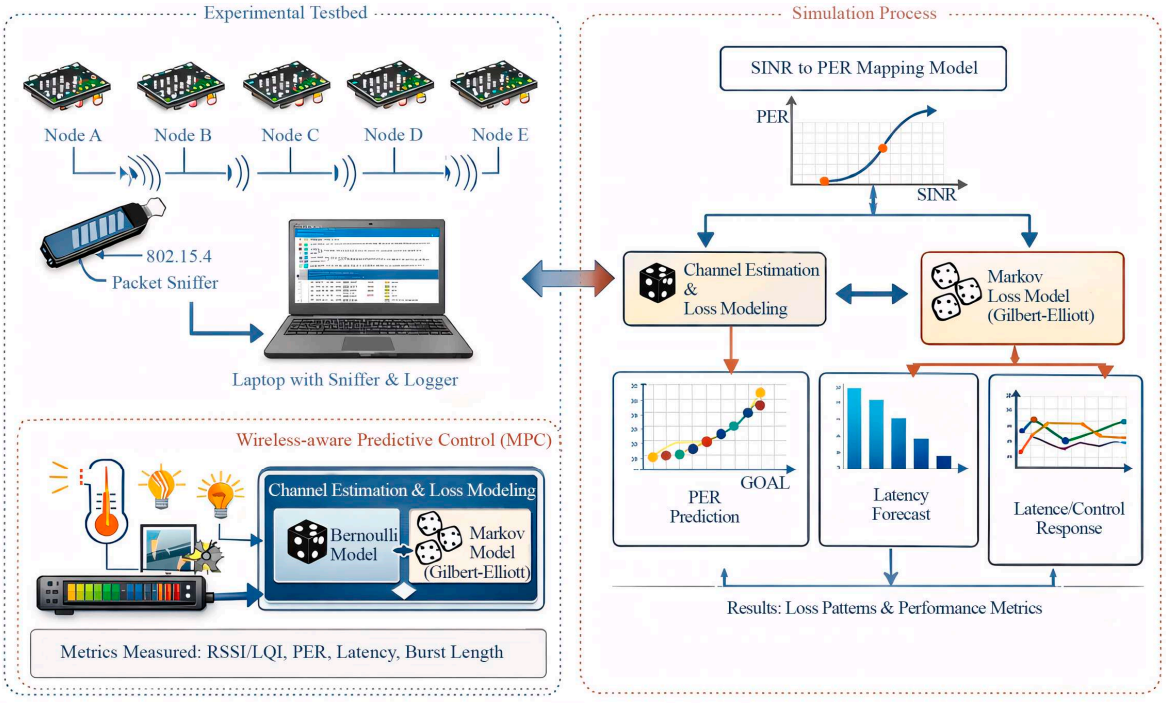

Fig. 1. Experimental testbed and integration of an SINR-based loss model with MPC

From these raw records, the metrics PER, latency, and burstiness are computed: PER is obtained by matching transmitted and received packets by sequence number; latency is computed for successfully delivered packets as $t_{rx} - t_{tx}$ and burstiness is quantified from consecutive loss runs (e.g., $E[N_{loss}]$ and $N_{loss,\max}$). Next, based on the measured RSSI/LQI (or an SINR proxy), the SINR → PER mapping is parameterized, and packet delivery is modeled using both an independent Bernoulli model and a temporally correlated finite-state Markov chain (FSMC, Gilbert-Elliott). The resulting loss/delay predictors are then incorporated into reliability-aware routing and an MPC-based algorithm that accounts for wireless-channel parameters, and the corresponding results are obtained.

4. 2. Physical-layer channel and link reliability model

Analysis is based on the transmitter characteristics for delay-sensitive wireless control applications. Single-antenna transceivers operating under the TSCH MAC protocol are considered and no retransmissions are assumed (i.e., no time diversity). The transmitted waveform follows the IEEE 802.15.4 2450 MHz DSSS PHY and uses half-sine pulse shaping, as commonly adopted in industrial wireless standards [16].

Channel and receiver impairments. The received signal quality is characterized by the instantaneous SINR

$$\mathrm{SINR} = \frac{P_r}{I + N_0}, \tag{1}$$

where P_r – the received signal power after propagation effects, and $I + N_0$ – the aggregated interference-plus-noise power. Large-scale attenuation is modeled using a two-slope path-loss law, while shadowing is modeled as log-normal. The combined impact of fading and interference is incorporated statistically through the SINR distribution [17].

Link reliability model. For a given SINR value, link reliability is determined using a standard SINR-to-PER mapping (or packet success probability) [18]. Packet delivery events are then modeled either as independent Bernoulli losses or as temporally correlated losses using a finite-state Markov chain [19]. These link-level statistics are subsequently used to construct end-to-end (E2E) loss metrics for multi-hop delivery and to support the routing/MPC co-design described in Section 5.

4. 3. Channel impairments of the signal

In this section, let's summarize the main propagation impairments affecting the received signal. Large-scale path loss is modeled by the standard log-distance law with a two-slope extension for the 2.4 GHz band

$$PL(d) = PL_0 + 10n\log_{10}\left(\frac{d}{d_0}\right), \tag{2}$$

where (d) (dB) – the large-scale path loss at the transmitter-receiver separation d(m); $PL_0 = PL(d_0)$ (dB) – the path loss at the reference distance d_0(m) (typically d_0=1m); n – the path-loss exponent (dimensionless); and log10(·)denotes the base-10 logarithm. In the two-slope extension, different exponents are used in the near and far regions, $n = n_1$ for $d \le db$ and $n = n_2$ for $d > db$, where db(m) – the breakpoint distance, and the far-region expression is defined to keep $PL(d)$ continuous at $d = d_b$.

Where n takes different values in near- and far-distance regions. The desired link also includes log-normal shadowing and residual power fluctuations after power control, while interfering signals follow free-space path loss with an additional obstacle attenuation factor. Multipath fading is neglected in the baseline setting due to highly absorptive industrial materials [20]. The resulting attenuation is used to compute P_r in the SINR model.

4. 4. Shadowing attenuation modeling

Shadowing is modeled as log-normal; equivalently, the shadowing attenuation $\beta_i(t)$ in dB is a Gaussian random variable with mean $\mu_{\beta i}$ and variance $\sigma^2_{\beta_i}$, consistent with indoor/industrial propagation studies [21]. For simplicity, the effect of shadowing on interfering links is captured through an additional mean attenuation term, while the variance is neglected in the baseline setting. These parameters are used to compute the received power P_r in the SINR model.

4. 5. Receiver input signal model

The channel impairments described above, together with AWGN and wideband interference, affect the signal of interest (SoI) at the receiver input. Accordingly, the received signal can be modeled as

$$y(t) = c(t)x(t) + i(t) + w(t), \tag{3}$$

where (t) – the transmitted IEEE 802.15.4 DSSS waveform, $i(t)$ denotes the aggregate interference, and $w(t)$ – the additive white Gaussian noise (AWGN) with one-sided power spectral density N_0 [22]. The effective channel gain $c(t)$ captures large-scale attenuation and residual fluctuations and is assumed approximately constant over one packet duration (block-fading), consistent with the IEEE 802.15.4-time scale [23].

5. Simulation studies and algorithm optimization results

5. 1. Evaluation of link reliability using the signal-to-interference-plus-noise ratio and packet error probability

Because temperature and humidity sensors and three surveillance cameras operate simultaneously in the warehouse, cross-technology interference (CTI) and nearby Wi-Fi traffic in the 2.4 GHz band directly affect the reliability of the wireless link. Experiments have shown that under CTI, time synchronization can be disrupted and the network join time can increase, which becomes especially critical when camera traffic is present. In TSCH networks, mechanisms such as scheduling, adaptive channel hopping, and channel blacklisting are used to mitigate interference and stabilize communication reliability. For low-power IEEE 802.15.4 networks, CTI not only increases packet corruption but also raises delay and jitter due to additional retransmissions [24–26]. Therefore, in this section, link reliability is quantified using SINR, and the packet error probability is computed through the SINR → BER → PER mapping. Following the channel model and assumptions stated in Section 4, the received signal at the receiver input is modeled as

$$y(t) = c(t)x(t) + V_u(t) + V_d(t) + W(t), \tag{4}$$

where $x(t)$ – the transmitted IEEE 802.15.4 DSSS waveform, $c(t)$ captures large-scale attenuation and slow variations (path loss, log-normal shadowing, and residual power-control error), V_u and $V_d(t)$ denote aggregated interference,

and $W(t)$ – the additive white Gaussian noise (AWGN) with one-sided power spectral density N_0 the average SINR of an L-bit packet for a given node ii can be written as follows.

For the IEEE 802.15.4 2.45 GHz DSSS PHY with O-QPSK modulation and half-sine pulse shaping, the BER/SER relations are standard; therefore, the packet error probability (PER) for an L-bit PHY packet is obtained using the well-known mapping

$$\overline{\gamma}_i = \frac{E_{s,i}}{I_i + N_0}, \quad E_{s,i} = c_i^2, \tag{5}$$

where E_s – the effective symbol energy of the desired signal (accounting for chip energy and channel gain), I_i – the equivalent interference power with respect to the signal of interest, and N_0 – the one-sided noise power spectral density.

For the IEEE 802.15.4 2.45 GHz DSSS PHY with O-QPSK modulation and half-sine pulse shaping, the BER/SER relations are standard; therefore, the packet error probability (PER) for an L-bit PHY packet is obtained using the well-known mapping

$$P_{pkt,i} = 1 - \left(1 - P_b\left(\gamma_i\right)\right)^L, \tag{6}$$

where $P_b(\gamma_i)$ – the bit error probability that accounts for half-sine pulse shaping and the PN sequences.

According to eq. (5), (6), the baseline distance-dependent reliability profile was obtained via Monte Carlo simulation. The transmitter-receiver separation for the 2.4 GHz radio signal was varied over the range $d = 1...100$ m, and for each distance d, $N_{MC} = 2000$ independent trials were performed. In each trial, the received power Pr, interference I, noise N, SINR, the bit error probability, and the packet error probability were computed. The plots in Fig. 2, a, b were then generated from the raw data by averaging, for each d, the resulting $\overline{\mathrm{SINR}}(d)$ and $\overline{P}_{pkt}(d)$ values.

Fig. 2, a indicates that the average signal-to-interference-plus-noise ratio decreases as the transmitter–receiver distance increases, reflecting a degradation of channel quality. Fig. 2, b shows that the packet error probability increases with distance, meaning that the likelihood of successful packet delivery decreases with increasing distance. Overall, increasing distance reduces channel quality and, consequently, increases packet errors; therefore, routing and control algorithms must explicitly account for channel conditions in order to maintain reliable communication.

Mechanisms such as scheduling, adaptive channel switching, and blacklists in TSCH networks are designed to stabilize communication quality by increasing resistance to interference [25]. In low-power networks, typical of IEEE 802.15.4, it has been shown that cross-technology interference (CTI) not only increases packet damage but also increases delay and jitter due to retransmissions [26]. Therefore, in warehouse automation (temperature/humidity monitoring and camera operation), the quality of control depends on the timely and reliable arrival of measurements, so a quantitative indicator describing channel reliability (e.g., BER based on SINR/PER and packet success probability) is important for control. In this work, let's take this indicator as the channel reliability and use it as an input parameter for subsequent joint design and adaptation decisions based on MPC.

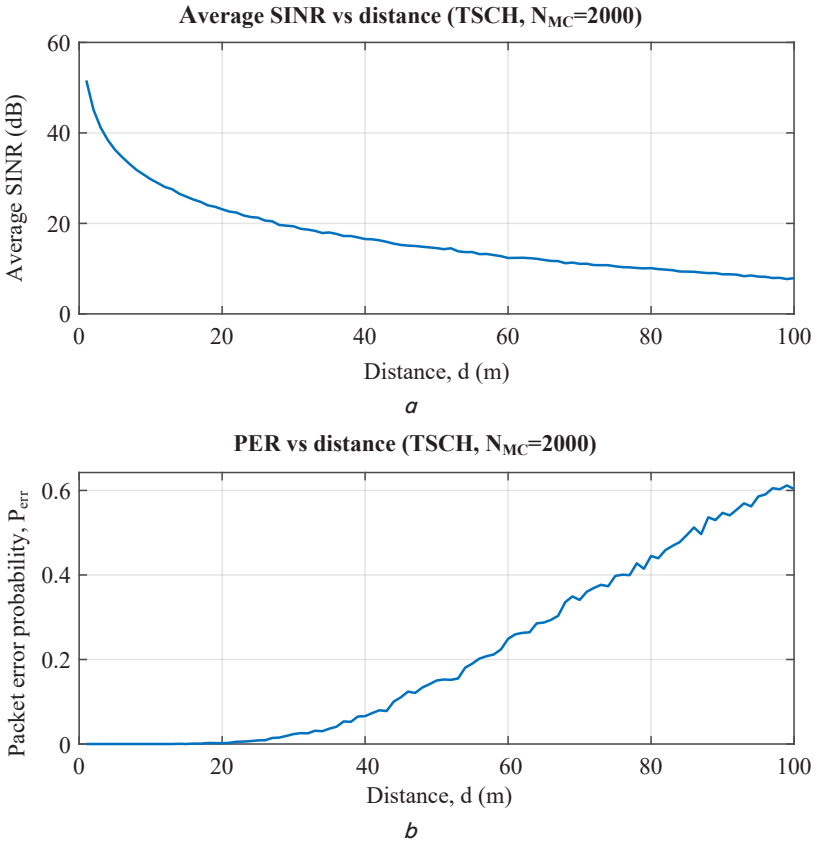

Fig. 2. Physical-layer link quality versus distance: a – average signal-to-interference-plus-noise ratio (average SINR) as a function of distance; b – packet error probability versus distance

5. 2. Analysis of packet loss in the single-hop scenario

In IEEE 802.15.4 based single-hop delivery, the packet loss probability depends not only on the physical channel quality but also on the MAC-layer access mechanism. Under contention-based CSMA/CA, the CCA and backoff procedure, as well as simultaneous attempts to access the channel, increase the collision probability and consequently intensify packet losses. This effect is quantitatively supported by an improved Markov analysis proposed for slotted CSMA/CA, which shows how the delivery probability changes when protocol parameters (backoff stages, CCA attempts, etc.) vary [27]. In addition, a study that provides an analytical model for IEEE 802.15.4 CSMA/CA clearly describes the impact of key protocol parameters and traffic load conditions on packet delivery performance, demonstrating that a significant portion of single-hop losses is inherently related to MAC-layer contention [28].

In contrast, under scheduled-access TSCH/TDMA, slotting substantially reduces collisions caused by simultaneous transmissions, while channel hopping mitigates interference effects and helps stabilize reliability. The robustness of TSCH under Wi-Fi interference has been specifically evaluated, and the results indicate that TSCH mechanisms (slotting + hopping) improve delivery reliability in the same environment [29]. Therefore, in this section, TDMA/TSCH and

CSMA/CA are compared for the same single-hop scenario, evaluating not only the average loss level but also its temporal structure (burst-like losses).

Single-hop setup. Five nodes are deployed in a 10m×10m area with a 10 m communication radius, ensuring single-hop connectivity to the sink. Each node transmits one packet every 5 s. The single-attempt success probability is

$$p_{s,i} = \mathbb{E}\left[1 - P_{pkt}(\gamma_i)\right], \quad (7)$$

where $P_{pkt,i}(\gamma_i)$ follows from the SINR-to-PER mapping in section 5. 1. Under TDMA/TSCH, interference is limited by scheduling; under CSMA/CA, concurrent access increases interference and reduces SINR, thus increasing losses.

Bernoulli loss model. If consecutive packets experience uncorrelated channel states, the delivery outcomes $X_k \in \{0,1\}$ are modeled as i.i.d.

$$\Pr(X_k = 1) = p_{s,i},\ \Pr(X_k = 0) = 1 - p_{s,i}. \quad (8)$$

FSMC loss model. To capture slow variations of shadowing and the resulting burst losses, it is possible to represent the channel by an M-state Markov chain Sk with transition matrix T

$$\Pr(S_{k+1} = j \mid S_k = i) = T_{ij},\ i, j = 1,\ldots,M. \quad (9)$$

Each state m is associated with a state-dependent $P_{pkt}(m)$, which makes $\{X_k\}$ temporally correlated.

In this section, single-hop packet losses under scheduled access (TDMA/TSCH) and contention-based access (CSMA/CA) are evaluated using two loss-process models: an independent Bernoulli model and an FSMC (finite-state Markov chain) model that captures time-correlated losses. For each node i and each packet index k, packet-level raw data were computed and stored in tabular form, including the received power $P_r(i, k)$, interference power $I(i, k)$, noise power $N_0(i, k)$, the corresponding SINR(i, k), the bit error probability $P_b(\gamma(i, k))$, the packet error probability $P_{pkt}(i, k)$, and the delivery indicator $X_k(i) \in \{0, 1\}$(where $X_k = 1$ indicates a successful delivery and $X_k = 0$ indicates a loss). Based on these raw data, the average packet loss probability P_{loss} and burst statistics were derived for each protocol/model pair; the resulting performance is shown in Fig. 3.

Fig. 3, *a* shows that the average packet loss probability is higher under CSMA/CA than under TDMA/TSCH, which is consistent with increased interference and collisions caused by concurrent channel access. Fig. 3, *b* illustrates that the FSMC model produces longer loss bursts than the Bernoulli model due to temporal correlation in shadow fading, resulting in larger burst metrics such as $[N_{loss}]$ and $N_{loss,\max}$. Overall, in the single-hop regime, scheduled access (TDMA/TSCH) provides higher reliability and more predictable delivery, whereas CSMA/CA exhibits increased loss and burstiness, which can degrade queuing behavior and effective delay.

The results shown in Fig. 3 indicate that TDMA/TSCH achieves a lower average packet loss probability than CSMA/CA and also reduces the clustering of losses (burstiness), i.e., both $\mathbb{E}[N_{loss}]$ and $N_{loss,\max}$ decrease. As a consequence, the measurement stream becomes more stable and the variability of delay and loss is reduced; therefore, the PER/E2E-loss and delay predictors used within the MPC operate more accurately and reliably.

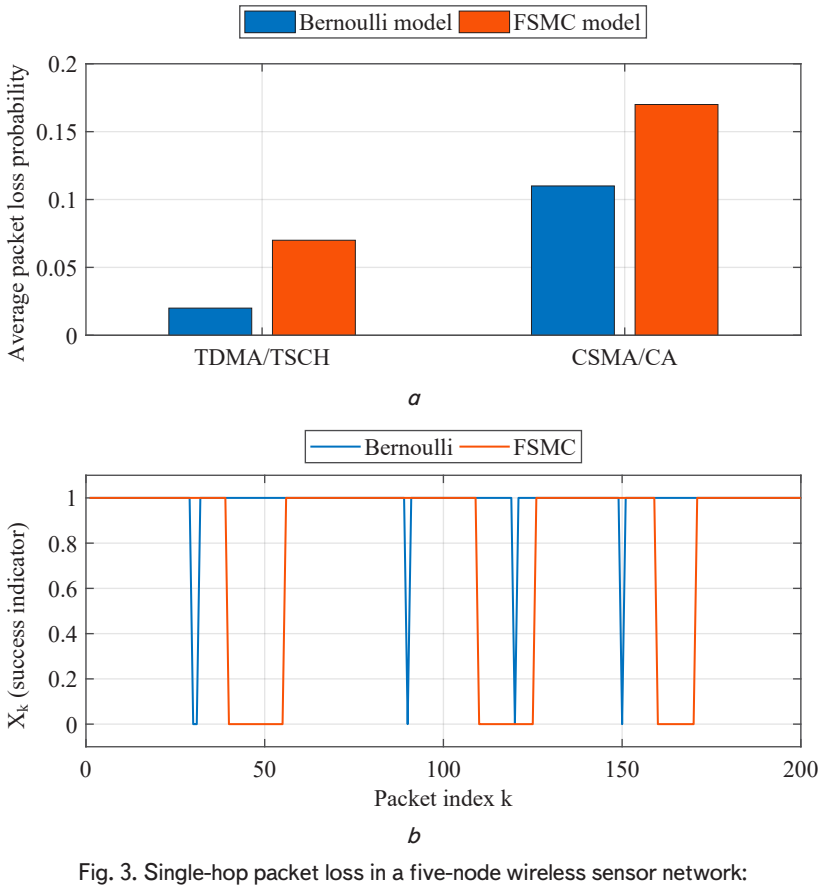

Fig. 3. Single-hop packet loss in a five-node wireless sensor network: *a* – average single-hop packet loss probability under TDMA/TSCH and CSMA/CA for the Bernoulli and FSMC models; *b* – sample realizations of the packet success process under TDMA/TSCH for the Bernoulli and FSMC models

5. 3. Multi-hop co-design routing and end-to-end packet loss

In multi-hop WSNs, end-to-end (E2E) delivery reliability is typically characterized by aggregating per-hop successful delivery, i.e., the E2E success probability is approximated as the product of the per-hop success probabilities. As a result, as the hop count increases, E2E performance naturally degrades rapidly: even if each link is reasonably reliable on average, the multiplicative effect across multiple hops reduces the overall delivery probability. Recent studies on long-range or multi-hop networks address this degradation by proposing reliability-aware routing as well as multipath and opportunistic forwarding, where link reliability and end-to-end delivery metrics are explicitly considered during route selection and traffic splitting [30].

Let's consider a packet routed over a path $P = \{n_0, n_1, \ldots n_H\}$ H hops. Under independent (Bernoulli) per-hop delivery, the E2E success probability is

$$P_{succ}^{\mathrm{E2E}} = \prod_{h=0}^{H-1} p_{s,n_h,n_{h+1}}, \quad (10)$$

and the corresponding E2E loss probability is

$$P_{loss}^{\mathrm{E2E}} = 1 - P_{succ}^{\mathrm{E2E}}, \tag{11}$$

where $p_{s,h} = 1 - P_{pkt,h}(\gamma_h)$ and $P_{pkt,h}(\gamma_h)$ follows from the SINR-to-PER mapping. If temporally correlated losses are represented by an FSMC (Section 5. 2), the route-level loss is evaluated using state-dependent packet error probabilities $P_{pkt}(m)$, which captures burst-loss effects in the reliability assessment.

From a WNCS perspective, packet losses can exhibit a "threshold" effect: if measurements arrive less frequently than required, the estimation quality can degrade sharply (with increasing error covariance), which directly impacts control performance. This strengthens the need to impose an explicit end-to-end reliability constraint P_{req}; in this sense, the traffic-splitting rule serves as a practical mechanism to keep the average E2E loss below the P_{req} threshold [31].

Reliability-constrained traffic splitting (co-design). Two alternative routes are compared: route A (fewer hops, lower per-hop SINR) and route B (more hops, higher per-hop SINR). Let $P_{loss,\mathrm{E2E}}^{A}$ and – $P_{loss,\mathrm{E2E}}^{B}$ be their E2E loss probabilities computed from (10), (11) (or from the FSMC-based evaluation). The routing co-design action is implemented by probabilistic traffic splitting: a fraction α of packets is sent via route A and $1 - \alpha$ via route B. The average E2E loss then becomes

$$\bar{P}_{loss}^{\mathrm{E2E}}(\alpha) = \alpha P_{loss,\mathrm{E2E}}^{A} + (1-\alpha) P_{loss,\mathrm{E2E}}^{B}. \tag{12}$$

Given the WNCS reliability requirement $\bar{P}_{loss}^{\mathrm{E2E}}(\alpha) \le P_{req}$, the feasible region of α\alphaα is obtained directly (a linear constraint). For example, if $P_{loss,\mathrm{E2E}}^{A} > P_{loss,\mathrm{E2E}}^{B}$, then

$$0 \le \alpha \le \min\left(1, \frac{P_{req} - P_{loss,\mathrm{E2E}}^{B}}{P_{loss,\mathrm{E2E}}^{A} - P_{loss,\mathrm{E2E}}^{B}}\right), \tag{13}$$

and otherwise the inequality reverses accordingly. This feasibility interval provides an explicit reliability-constrained routing decision rule that is subsequently embedded into the routing/MPC co-design procedure in Section 5. 4.

Fig. 4, *a* shows that the E2E loss increases rapidly with hop count H for identical per-hop reliability, which motivates limiting hop count or improving per-hop link quality. Fig. 4, *b* demonstrates that traffic splitting yields a controllable reliability margin: for a non-empty range of α, the average E2E loss remains below P_{req}, enabling reliability-aware route selection within the co-design framework.

Fig. 4, *a* shows that the end-to-end (E2E) loss increases rapidly as the hop count H grows, meaning that reliability degrades quickly for multi-hop routes. Fig. 4, *b* demonstrates that by splitting traffic between two routes (α), the average loss can be kept below the reliability requirement

Preq: for a feasible interval of α, the condition $\bar{P}_{loss}^{\mathrm{E2E}}(\alpha) \le P_{req}$ holds. The key significance and advantage of this study is that it does not discuss reliability only qualitatively; instead, it provides a solution that enables routing decisions to be governed by an explicit quantitative rule. The admissible range of α is directly embedded into the co-design step to jointly configure route selection and the MPC settings. As a result, one of the most critical WNCS requirements stable and explicitly guaranteed communication reliability is supported, reducing measurement dropouts and the increase in effective delay caused by higher loss rates. This approach enables efficient use of network resources (routes/traffic) while preserving control performance (tracking accuracy).

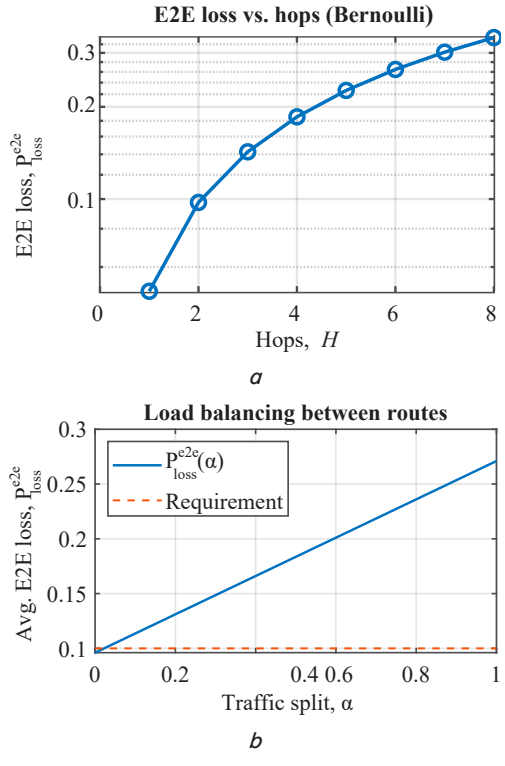

Fig. 4. Multi-hop end-to-end loss and reliability-constrained traffic splitting: *a* – $P_{loss,\mathrm{E2E}}$ versus hop count H; *b* – average E2E loss $\bar{P}_{\mathrm{loss}}^{\mathrm{E2E}}(\alpha)$ versus traffic split α with the requirement P_{req} (dashed line)

5. 4. MPC-based joint adaptation of wireless communication parameters and control

Based on the previously presented WNCS interaction architecture and the considered experimental/simulation scenario (IEEE 802.15.4-based multi-hop delivery and the measurement-control closed loop), simulations are conducted using the pre-obtained values (parameters). On this basis, the results obtained for the MPC-based co-design that accounts for wireless-channel parameters are presented. The main focus here is to demonstrate how packet loss and time-varying communication delay, quantitatively evaluated via the loss/delay predictors obtained from the channel, affect the closed-loop control quality, and to analyze the results achieved by jointly adapting the control and communication parameters within the MPC framework in order to mitigate these effects.

In the simulation scenario, five nodes deployed in a 10×10 m area are considered; measurements are taken every 5 s and delivered to the controller in a time-slotted manner, which introduces time-varying delay. The MAC layer can be TSCH/CSMA/CA or TDMA. For closed-loop evaluation, the plant state $xp(k)$ is normalized to [0, 1], and the target value is chosen as a step reference $r = 0.5$ (normalized units). For comparison, in addition to the proposed MPC scheme, an LQR baseline controller is also used.

In this work, the model predictive control problem is formulated using an augmented state that accounts for wireless-channel effects: $x(k) = [x_p(k), q(k)]$ where $x_p(k)$ is the plant state and $q(k) \in [0,1]$ is an indicator that summarizes the current channel quality (e.g., a normalized measure derived from SINR/channel gain or the probability of successful

access). The communication parameters are included in the control vector and selected as $u(k) = [P_{tx}(k), T_s(k), N_{ret}(k)]$: the transmit power, the sampling/transmission period, and the number of retransmissions jointly determine the reliability-delay-energy trade-off. This formulation is well motivated: prior work has shown that jointly designing channel-aware scheduling and packet-based predictive control is necessary to compensate for packet losses and ensure stability, and it analyzes how stability depends on the prediction horizon and the successful access probability [32].

At each time step, the link packet error probability $P_p(\gamma)$ is evaluated from the SINR-based mapping in (5), (6) (Fig. 2), yielding the link success probability $p_s(k) = 1 - P(\gamma(k))$. Temporal loss behavior is captured using the Bernoulli and FSMC models in (8), (9) (Fig. 3). For multi-hop routes, the end-to-end reliability is computed using (10), (11) and, when applicable, the reliability-constrained traffic-splitting rule in (12), (13) (Fig. 4). These predictors are then used as inputs to the MPC-based co-design in this subsection. First, BER is obtained from SINR values using the standard mapping adopted for IEEE 802.15.4, and then the packet error probability (PER) $P_{pkt}(\gamma)$ is derived. Based on PER, the single-link success probability is computed as $p_s(k) = 1 - P_{pkt}(\gamma(k))$. For a multi-hop route, the end-to-end (E2E) reliability is determined using the hop-wise aggregation rule presented in Section 5. 3, i.e., the per-hop *ps*ps values are combined to obtain the E2E success probability and the corresponding E2E loss probability. In this section, these results are evaluated online through the channel-quality indicator $q(k)$ and used as inputs to the PER/E2E-loss predictor within the MPC.

Taking the constraints into account, it is possible to formulate the model predictive control (MPC) objective function and the corresponding optimization problem. The WNCS requirements are: $P_{loss}^{\mathrm{E2E}}(k) \le P_{\max}$ (e.g., 1–5%), $D^{\mathrm{E2E}}(k) \le D_{\max}$ (e.g., 100–200 ms). MPC optimization problem: at each time step k, MPC solves the following problem over the prediction horizon N_p

$$\min_{\{u(k),\ldots,u(k+N_p-1)\}} \sum_{j=0}^{N_p-1} \begin{pmatrix} w_p\left(x_p(k+j)-\right)^2 + \\ -r \\ +w_e \tilde{P}_{tx}^2(k+j)+ \\ +w_d \tilde{D}^2(k+j) \end{pmatrix}. \quad (14)$$

The first term $w_p(x_p - r)^2$ represents the tracking accuracy of the plant state with respect to the reference r. The second term $w_e \tilde{P}_{tx}^2$ penalizes the transmit power (energy consumption) and prevents unnecessary increases of P_{tx} when the channel conditions improve. The third term $w_d \tilde{D}^2$ penalizes the end-to-end delay and supports satisfying the timeliness requirement by keeping the delay away from the limit $D_{\max}$. The normalized variables $\tilde{P}_{tx} = P_{tx}/P_{tx,\max}$ and $\tilde{D} = D^{e2e}/D_{\max}$ bring quantities with different physical units to a common scale and allow controlling the trade-off via the weighting coefficients. In this way, MPC ensures the selection of $\{P_{tx}(k), T_s(k), N_{retx}(k)\}$ that satisfies the constraints $P_{loss}^{\mathrm{E2E}} \le P_{\max}$ and $D^{\mathrm{E2E}} \le D_{\max}$, while maintaining the compromise between tracking-energy-delay.

Constraints. The optimization in (14) is subject to WNCS-level quality-of-service requirements that enforce reliability and timeliness over the prediction horizon. Specifically, the end-to-end packet-loss probability must not exceed $P_{\max}$, and the end-to-end delay must remain below $D_{\max}$. In addition, the communication parameters are selected from discrete sets consistent with IEEE 802.15.4 implementation limits (e.g., admissible power levels, sampling periods, and retransmission counts). Accordingly, the constraints are given by

$$P_{loss}^{\mathrm{E2E}}(k+j) \le P_{\max},\ D^{\mathrm{E2E}}(k+j) \le D_{\max},\ j = 0,\ldots,N_p - 1, \quad (15)$$

$$P_{tx}(k) \in \mathcal{P},\ T_s(k) \in \mathcal{T},\ N_{retx}(k) \in \mathcal{N}, \quad (16)$$

where $\mathcal{P}$, $\mathcal{T}$, $\mathcal{N}$ are discrete feasible sets consistent with IEEE 802.15.4 constraints (e.g., 0/5/10 dBm; 0.05/0.1/0.2 s; 0/1/2).

Fig. 5 shows the continuous approach of the closed-loop plant state $x_p(k)$ to the given reference value using the proposed MPC algorithm. Despite network loads and packet error probability, the joint parameter selection approach based on MPC ensures the stability of the system and the required transient response. Given that the control action only affects the plant during steps where packets are successfully delivered, the correct selection of WNCS parameters plays a crucial role.

At each discrete step k, the MPC uses the current state to solve an optimization problem and jointly selects the WNCS communication parameters along with the control action: the transmission power (k), the sampling period $T_s(k)$, and the maximum allowed number of retransmissions $N_{\max}(k)$. These parameters determine the packet delivery reliability in the network model. Therefore, the control action is applied to the plant only when the packet is successfully delivered. The resulting trajectory (k) is compared with the reference value, forming the dynamic response plot shown in Fig. 6.

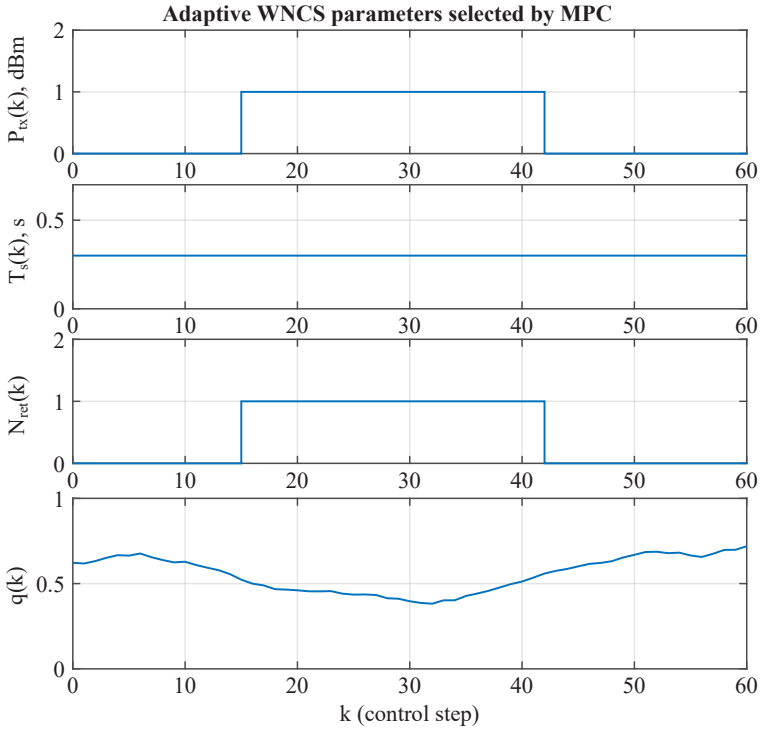

Fig. 5. Dynamics of the WNCS parameters selected by model predictive control: $P_{tx}(k)$ — transmit power (k) dBm; $T_s(k)$ — sampling/transmission period, s; maximum number of retransmissions; $x_p(k)$ — channel quality indicator

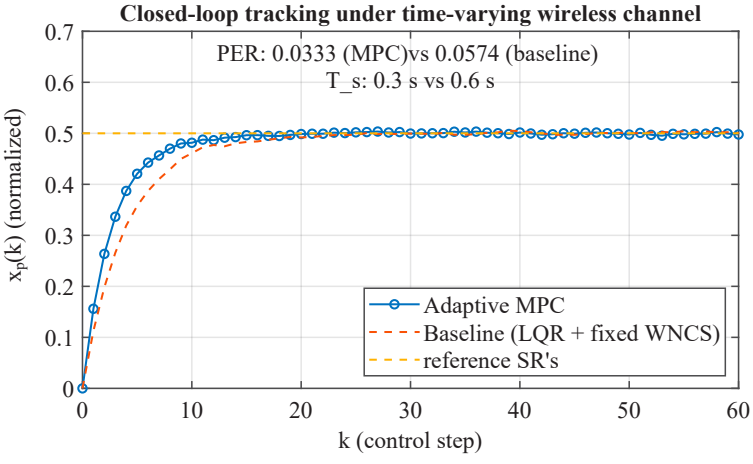

Fig. 6. Dynamic response of the system under the proposed model predictive control-based co-design with adaptive wireless networked control system parameters

Fig. 6 clearly demonstrates the practical advantages of the proposed MPC based co-design algorithm that accounts for wireless communication parameters. Even under time-varying channel conditions, the plant state $x_p(k)$ converges to the reference r in a stable and smooth manner; the transient response remains stable despite packet losses and delay variations. Compared with the baseline approach using fixed network settings, the co-design solution also improves control performance in quantitative terms: the packet error rate (PER) decreases from 0.0445 to 0.0366 (about a 17.8% reduction), the average delay drops from 0.200 s to 0.117 s (about a 41.7% reduction), and the integral tracking error indicator (LAE) is reduced from 0.0969 to 0.0484 (about a 50% improvement). In addition, the algorithm accelerates the response by keeping the sampling period T_s at 0.3 s instead of 0.6 s, without compromising stability.

Therefore, the main achievement of Section 5. 4 is that, by jointly adapting the communication parameters (P_{tx}, T_s, N_{ret}) together with the control action, the proposed method achieves more stable tracking, lower delay, and improved reliability while meeting the WNCS reliability and timeliness requirements. This confirms that the co-design step, based on the feasible parameter region, turns parameter selection into a concrete and effective mechanism in practice.

6. Discussion of results for model predictive control-controlled wireless networked control systems

Link-level reliability is quantified by evaluating the instantaneous SINR from the received signal and the aggregated interference-plus-noise according to (1)–(4). For the IEEE 802.15.4 2.45 GHz DSSS PHY, the corresponding BER is obtained from SINR using (5), and the packet error probability for an L-bit packet is computed via (6). The Monte Carlo results in Fig. 2, *a*, *b* confirm the expected trend: as the transmitter–receiver distance increases, SINR decreases and the packet error probability increases. This provides a physically interpretable link-reliability basis that is subsequently used to form end-to-end loss metrics through the hop-wise aggregation in (10), (11) and to parameterize the MPC co-design optimization and constraints in (15), (16).

The single-hop loss behavior under scheduled access and contention-based access is summarized in Fig. 3. For the same physical-layer reliability $P_{pkt}(\gamma)$ and the corresponding single-attempt success model in (7), TDMA/TSCH yields a lower average loss probability than CSMA/CA (Fig. 3, *a*), which is consistent with deterministic slot allocation that suppresses contention-driven collisions, whereas CSMA/CA is affected by backoff and simultaneous channel access attempts. The temporal structure of losses is captured by the Bernoulli and FSMC formulations in (8), (9): compared with the i.i.d. Bernoulli case, the FSMC model produces longer loss runs, reflected by larger burst metrics $E[N_{loss}]$ and $N_{loss,\max}$ (Fig. 3, *b*). This distinction is control-relevant because burst losses imply consecutive missed measurements and a higher effective latency than isolated packet errors.

End-to-end (E2E) loss over an H-hop route is evaluated by aggregating the per-hop delivery probabilities using the hop-wise Bernoulli formulation in (10), (11). The results in Fig. 4, *a* show that E2E loss increases markedly with hop count: in the considered setup it rises from approximately 3% to approximately 32% as H grows from 1 to 8, which motivates either limiting the hop count or improving per-hop link quality. Reliability-aware routing is further quantified via the traffic-splitting model in (12): the average E2E loss depends linearly on the split coefficient α, and enforcing the reliability requirement $\bar{P}_{loss,E2E}(\alpha) \le P_{req}$ yields a simple feasible interval for α given in (13), as illustrated in Fig. 4, *b*. This provides an explicit quantitative rule that links route selection (or route mixing) to a target reliability constraint.

The closed-loop co-design performance is summarized in Fig. 5, 6. At each time step k, the MPC solves the optimization problem in (15) using the augmented state $x(k) = [x_p(k), q(k)]$ where $q(k)$ represents the channel-quality indicator derived from the reliability predictor, and it jointly selects the decision variables $u(k) = [P_{tx}(k), T_s(k), N_{ret}(k)]$ under the prescribed reliability and timeliness constraints (E2E loss and delay bounds). Fig. 5 illustrates how the selected communication parameters adapt over time in response to channel-quality variations, while Fig. 6 confirms stable reference tracking under packet loss and time-varying delay. Compared with the fixed-parameter LQR baseline, the MPC-based co-design reduces the E2E packet error rate from 4.45% to 3.66%, decreases the average delay from 0.20 s to 0.12 s, and improves the integrated absolute error from 0.0969 to 0.0484 (50% reduction). The E2E loss remains within the 5% requirement in the considered scenario, and no overshoot is observed. Overall, these results indicate that reliability-predictor-driven adaptation of P_{tx}, T_s, and N_{ret} is effective for maintaining closed-loop performance under wireless-induced losses and delays.

Compared with MAC-oriented studies that optimize throughput or delay in isolation, the proposed framework connects physical-layer SINR variations, MAC behavior and routing decisions directly to E2E loss and closed-loop control quality. Link and E2E loss expressions are parameterized by physical quantities (path loss, shadowing, interference), which makes the reliability model transparent and interpretable.

Unlike approaches that treat the network as a fixed disturbance and compensate losses only on the controller side, the network parameters P_{tx}, T_s, N_{retx} and the routing split α are explicit decision variables in the MPC problem. This joint treatment enables simultaneous satisfaction of reliability/de-

lay constraints and improvement of control performance. The quantitative gains over the LQR baseline (17.8% reduction in packet error rate, 41.7% reduction in average delay, 50% reduction in tracking error) illustrate this advantage.

In addition, the proposed traffic-splitting region $\{\alpha: \overline{P}_{loss,E2E}(\alpha) \le P_{req}\}$, provides a simple, reliability-based rule for using multiple routes, which is not present in most existing WNCS works. A key gap identified in the literature is the lack of a unified, physically grounded end-to-end (E2E) loss-and-delay model for IEEE 802.15.4-based wireless networked control systems that can be used directly in controller synthesis. The present study addresses this gap for a well-defined class of systems and operating conditions considered in the paper.

First, a SINR-based PHY model is linked to BER/PEP and packet error probability, forming the basis for link-level reliability. Second, Bernoulli and FSMC models provide both independent and bursty loss descriptions under TDMA/TSCH and CSMA/CA. Third, per-hop loss probabilities are combined into E2E loss for multi-hop routes, and a reliability-constrained traffic-splitting strategy is derived. Finally, the resulting loss and delay predictors are embedded into the MPC formulation, which enforces E2E loss and delay constraints and improves closed-loop performance in simulation.

Thus, the study offers a concrete SINR → loss → control chain for IEEE 802.15.4-based WNCS and demonstrates its effectiveness under the chosen assumptions. However, the analysis is limited to specific topologies, traffic patterns and parameter ranges, and is validated only in simulation. Therefore, the general problem is addressed partially rather than fully resolved for all industrial scenarios.

This study has several limitations that define the scope and applicability of the obtained results. First, the IEEE 802.15.4 channel characterization relies on stationary path-loss and shadowing statistics and uses a simplified interference description; therefore, the reported reliability and delay trends may differ in industrial environments with highly time-varying or heterogeneous interference. Second, the comparison of TDMA/TSCH and CSMA/CA is performed without explicit consideration of implementation-level effects such as clock drift and resynchronization errors, vendor-specific backoff behavior, and cross-technology interference dynamics, which can affect collision probability, latency, and burstiness. Third, the multi-hop evaluation is restricted to a small set of routes and represents route diversity using a scalar traffic-splitting coefficient; thus, the presented routing conclusions do not directly generalize to large-scale networks with dynamic topology changes and adaptive routing. Fourth, the reported MPC co-design performance is obtained under simulation and depends on the fidelity of the plant model and on the timely availability of the channel-quality indicator $q(k)$; sensitivity to model mismatch and estimation delay is not quantified in this work. Finally, a key shortcoming is the lack of hardware testbed validation: the results are simulation-based, and implementation details required for full reproducibility (e.g., complete parameter tables, solver settings, and random seeds) should be explicitly reported and complemented by raw measurement traces in future work. Consequently, the proposed framework is most applicable to IEEE 802.15.4-based WNCS with relatively static topologies and traffic, identifiable channel/interference statistics, and sufficient computational resources for real-time MPC execution.

Future research should first focus on experimental validation of the proposed framework on an IEEE 802.15.4 hardware testbed, explicitly accounting for realistic interference, synchronization imperfections, and hardware constraints, in order to refine the channel and loss models and to verify the MPC-based co-design under real operating conditions. The approach can then be extended to larger, dynamically routed multi-hop networks with heterogeneous links and time-varying interference, which will likely require online identification of FSMC parameters and SINR statistics, combining data-driven and model-based techniques. In addition, more advanced control formulations, such as robust or chance-constrained MPC, should be explored to handle uncertainty in loss and delay predictions and to provide probabilistic performance guarantees. Finally, the joint use of MPC-based co-design with complementary mechanisms (e.g., forward error correction, packet bundling, adaptive quantization) and the study of their combined impact on reliability and control performance constitute promising directions for further investigation.

7. Conclusion

1. The SINR/BER-based model shows that as distance increases, received power and average SINR decrease, while PER grows nonlinearly. This means that longer hops lead to higher packet error rates, so reliable IEEE 802.15.4-based WNCS operation requires bounded hop lengths and, when needed, multi-hop routing with short hops.

2. In the single-hop case, TDMA/TSCH yields lower loss and more stable delay than CSMA/CA, because time slots are pre-assigned and collisions are largely avoided, whereas CSMA/CA suffers from contention and random backoff. Therefore, TDMA/TSCH is preferable for control applications where timing determinism and low delay variability are important.

3. For multi-hop networks, the analysis shows that end-to-end loss grows rapidly with hop count, even when per-hop quality is high. Reliability can be adjusted by splitting traffic between routes with different quality: increasing the share on the better route reduces the overall loss. This provides a simple, quantitative way to use routing and traffic splitting to satisfy a given end-to-end loss constraint.

4. The proposed MPC-based co-design jointly adapts transmit power, sampling period, retransmissions, and routing/MAC parameters to meet end-to-end loss and delay requirements. When tracking error is large, MPC temporarily increases reliability (higher power, more retransmissions, shorter period); as the system stabilizes, it reduces these settings to save energy and bandwidth. Compared with a fixed-parameter LQR baseline, this yields lower packet error rate, lower average delay, and about 50% reduction in tracking error, and explicitly links an end-to-end reliability model with controller synthesis.

Conflict of interest

The authors declare that they have no conflict of interest related to this study –financial, personal, authorship, or otherwise – that could influence the study and the results presented in this paper.

Financing

This study was carried out at the "Electronics, Space Engineering, and Telecommunication Technologies Laboratory" of Satbayev University and forms a part of the master's dissertation work in the field of wireless networked control systems. The study was conducted without external funding.

Data availability

The data supporting the findings of this study will be made available on reasonable request from the corresponding author.

Use of artificial intelligence tools

ChatGPT (GPT-5.2 Thinking) was used to a limited extent for proofreading the English text, including grammar, spelling, and punctuation checks.

The AI tool was used only in preparing the English-language text (e.g., in the Abstract, Introduction/Literature Review, Aim and Objectives, and Data Availability sections), specifically for proofreading and correcting grammar, spelling, punctuation, and improving overall clarity and logical consistency.

The AI tool was used only for language-related tasks:

1) proofreading the English text;

2) correcting grammar, spelling, punctuation, and minor sentence-level errors;

3) improving readability and logical consistency without changing the technical meaning;

4) checking consistency of terminology and notation across the English sections. The AI tool was not used to develop scientific ideas, perform theoretical analysis, design algorithms, run simulations, interpret results, or write the study conclusions.

The authors manually reviewed the AI-suggested edits and verified that the scientific meaning, terminology, formulas, notation, and references remained unchanged. They made corrections where necessary and finalized the manuscript through full author review.

The AI tool did not influence the scientific conclusions of the study. It was used only for English-language proofreading (grammar, spelling, and punctuation), while all analyses, results, and conclusions were produced and validated by the authors.

Authors' contributions

Anar Khabay: Conceptualization, Methodology, Modeling, Formal analysis, Software, Investigation, Validation, Visualization, Writing – original draft; **Ainur Ormanbekova**: Conceptualization, Methodology, Supervision, Validation, Writing – review & editing; **Yerkebulan Tuleshov**: Software, Modeling, Investigation, Visualization, Data curation; **Nurlan Sarsenbayev**: Investigation, Validation, Resources, Project administration; **Zhazira Julayeva**: Formal analysis, Data curation, Resources, Documentation; **Serikbek Ibekeyev**: Investigation, Validation, Resources, Formal analysis; **Maral Abulkhanova**: Literature review, Formal analysis, Writing – review & editing; **Askhat Tlegenov**: Investigation, Software, Formal analysis, Data curation; **Magzhan Igen**: Software, Investigation, Visualization, Integration, Writing – review & editing.

References

1. Pezzutto, M., Dey, S., Garone, E., Gatsis, K., Johansson, K. H., Schenato, L. (2024). Wireless control: Retrospective and open vistas. Annual Reviews in Control, 58, 100972. https://doi.org/10.1016/j.arcontrol.2024.100972
2. Hamdan, M. M., Mahmoud, M. M. (2022). Analysis and Challenges in Wireless Networked Control System: A Survey. International Journal of Robotics and Control Systems, 2 (3), 492–522. https://doi.org/10.31763/ijrcs.v2i3.731
3. Huang, K., Liu, W., Li, Y., Savkin, A., Vucetic, B. (2020). Wireless Feedback Control With Variable Packet Length for Industrial IoT. IEEE Wireless Communications Letters, 9 (9), 1586–1590. https://doi.org/10.1109/lwc.2020.2998611
4. Liu, Y., Wang, J., Gomes, L., Sun, W. (2021). Adaptive Robust Control for Networked Strict-Feedback Nonlinear Systems with State and Input Quantization. Electronics, 10 (22), 2783. https://doi.org/10.3390/electronics10222783
5. Shi, T., Guan, Y., Zheng, Y. (2022). Model predictive control of networked control systems with disturbances and deception attacks under communication constraints. International Journal of Robust and Nonlinear Control, 35 (7), 2717–2735. https://doi.org/10.1002/rnc.6363
6. Kuatova, M., Tuleshov, A., Baurzhan, A., Jomartov, A., Tuleshov, Y., Sayakov, O. (2025). Development and Validation of An Automated Crank Press System Integrating the Stephenson II Six-Bar Linkage and Model Predictive Control. ES Materials & Manufacturing. https://doi.org/10.30919/mm1799
7. Lee, M.-F. R., Chiu, F.-H. S., Huang, H.-C., Ivancsits, C. (2013). Generalized Predictive Control in a Wireless Networked Control System. International Journal of Distributed Sensor Networks, 9 (12), 475730. https://doi.org/10.1155/2013/475730
8. Florenzan Reyes, L. F., Smarra, F., Lun, Y. Z., D'Innocenzo, A. (2021). Learning Markov models of fading channels in wireless control networks: a regression trees based approach. 2021 29th Mediterranean Conference on Control and Automation (MED), 232–237. https://doi.org/10.1109/med51440.2021.9480310
9. Kim, M.-J., Lee, H.-I., Choi, J.-H., Lim, K. J., Mo, C. (2022). Development of a Soil Organic Matter Content Prediction Model Based on Supervised Learning Using Vis-NIR/SWIR Spectroscopy. Sensors, 22 (14), 5129. https://doi.org/10.3390/s22145129
10. Silva, C. A. G. da, Santos, E. L. dos (2023). A Compensation Model for Packet Loss Using Kalman Filter in Wireless Network Control Systems. Energies, 16 (8), 3329. https://doi.org/10.3390/en16083329
11. Yue, X., Liu, Y. (2022). Performance Analysis of Intelligent Reflecting Surface Assisted NOMA Networks. IEEE Transactions on Wireless Communications, 21 (4), 2623–2636. https://doi.org/10.1109/twc.2021.3114221
12. Jia, Y., Ye, C., Cui, Y. (2020). Analysis and Optimization of an Intelligent Reflecting Surface-Assisted System With Interference. IEEE Transactions on Wireless Communications, 19 (12), 8068–8082. https://doi.org/10.1109/twc.2020.3019088

13. Orea-Flores, I. Y., Rivero-Angeles, M. E., Gonzalez-Ambriz, S.-J., Anaya, E. A., Saleem, S. (2024). Performance Analysis of Wireless Sensor Networks Using Damped Oscillation Functions for the Packet Transmission Probability. Computers, 13 (11), 285. https://doi.org/10.3390/computers13110285
14. Zila, A., Ouchatti, A., Mouzouna, Y. (2025). Exploring Node Failure and Packet Loss in Wireless Sensor Networks: A Comprehensive Simulation Analysis. International Journal of Communication Systems, 38 (13). https://doi.org/10.1002/dac.70174
15. Lun, Y. Z., Rinaldi, C., D'Innocenzo, A., Santucci, F. (2024). Co-Designing Wireless Networked Control Systems on IEEE 802.15.4-Based Links Under Wi-Fi Interference. IEEE Access, 12, 71157–71183. https://doi.org/10.1109/access.2024.3402082
16. Vayssade, T., Azais, F., Latorre, L., Lefevre, F. (2019). Low-Cost Digital Test Solution for Symbol Error Detection of RF ZigBee Transmitters. IEEE Transactions on Device and Materials Reliability, 19 (1), 16–24. https://doi.org/10.1109/tdmr.2019.2898769
17. Díez, V., Arriola, A., Val, I., Velez, M. (2020). Reliability evaluation of point-to-point links based on IEEE 802.15.4 physical layer for IWSAN applications. AEU - International Journal of Electronics and Communications, 113, 152967. https://doi.org/10.1016/j.aeue.2019.152967
18. Barac, F., Gidlund, M., Zhang, T. (2014). Scrutinizing Bit- and Symbol-Errors of IEEE 802.15.4 Communication in Industrial Environments. IEEE Transactions on Instrumentation and Measurement, 63 (7), 1783–1794. https://doi.org/10.1109/tim.2013.2293235
19. Chen, D., Zhuang, Y., Huai, J., Sun, X., Yang, X., Awais Javed, M. et al. (2021). Coexistence and Interference Mitigation for WPANs and WLANs From Traditional Approaches to Deep Learning: A Review. IEEE Sensors Journal, 21 (22), 25561–25589. https://doi.org/10.1109/jsen.2021.3117399
20. Yang, D., Xu, Y., Gidlund, M. (2011). Wireless Coexistence between IEEE 802.11- and IEEE 802.15.4-Based Networks: A Survey. International Journal of Distributed Sensor Networks, 7 (1), 912152. https://doi.org/10.1155/2011/912152
21. Yu, Y.-S., Chen, Y.-S. (2020). A Measurement-Based Frame-Level Error Model for Evaluation of Industrial Wireless Sensor Networks. Sensors, 20 (14), 3978. https://doi.org/10.3390/s20143978
22. Brown, J., Roedig, U., Boano, C. A., Romer, K. (2014). Estimating packet reception rate in noisy environments. 39th Annual IEEE Conference on Local Computer Networks Workshops, 583–591. https://doi.org/10.1109/lcnw.2014.6927706
23. Satoh, D., Kobayashi, K., Yamashita, Y. (2018). MPC-based Co-design of Control and Routing for Wireless Sensor and Actuator Networks. International Journal of Control, Automation and Systems, 16 (3), 953–960. https://doi.org/10.1007/s12555-017-0170-7
24. Kidane, Z. M., Dargie, W. (2025). Impact of Cross Technology Interference on Time Synchronization and Join Time in Low-Power Wireless Networks. https://doi.org/10.2139/ssrn.5119414
25. Balbi, M., Doherty, L., Watteyne, T. (2025). A comprehensive survey on channel hopping and scheduling enhancements for TSCH networks. Journal of Network and Computer Applications, 238, 104164. https://doi.org/10.1016/j.jnca.2025.104164
26. Kidane, Z. M., Dargie, W. (2025). Cross-technology interference: detection, avoidance, and coexistence mechanisms in the ISM bands. CCF Transactions on Pervasive Computing and Interaction, 7 (3), 356–375. https://doi.org/10.1007/s42486-025-00185-0
27. Wen, H., Lin, C., Chen, Z.-J., Yin, H., He, T., Dutkiewicz, E. (2009). An Improved Markov Model for IEEE 802.15.4 Slotted CSMA/CA Mechanism. Journal of Computer Science and Technology, 24 (3), 495–504. https://doi.org/10.1007/s11390-009-9240-5
28. Kim, S., Kim, B.-S., Kim, K. H., Kim, K.-I. (2019). Opportunistic Multipath Routing in Long-Hop Wireless Sensor Networks. Sensors, 19 (19), 4072. https://doi.org/10.3390/s19194072
29. Marelli, D. E., Sui, T., Rohr, E. R., Fu, M. (2019). Stability of Kalman filtering with a random measurement equation: Application to sensor scheduling with intermittent observations. Automatica, 99, 390–402. https://doi.org/10.1016/j.automatica.2018.11.003
30. Li, P., Zhao, Y.-B., Kang, Y. (2022). Integrated Channel-Aware Scheduling and Packet-Based Predictive Control for Wireless Cloud Control Systems. IEEE Transactions on Cybernetics, 52 (5), 2735–2749. https://doi.org/10.1109/tcyb.2020.3019179
31. Liu, W., Quevedo, D. E., Li, Y., Johansson, K. H., Vucetic, B. (2022). Remote State Estimation With Smart Sensors Over Markov Fading Channels. IEEE Transactions on Automatic Control, 67 (6), 2743–2757. https://doi.org/10.1109/tac.2021.3090741
32. Girgis, A. M., Park, J., Bennis, M., Debbah, M. (2021). Predictive Control and Communication Co-Design via Two-Way Gaussian Process Regression and AoI-Aware Scheduling. IEEE Transactions on Communications, 69 (10), 7077–7093. https://doi.org/10.1109/tcomm.2021.3099156